

Uniform Porous Nanospheres of Discrete Shape-persistent Organic Cage Compounds

Markus W. Schneider,^a Lorenz G. Lechner^b and Michael Mastalerz^{*a}

Supporting Information

General Remarks: Melting points (not corrected) were measured with a Büchi Melting Point B-545. IR-Spectra were recorded as KBr-pellets (solids) or between two NaCl disks (liquids) on a Perkin Elmer Spectrum 2000 FT-IR spectrometer. NMR spectra were recorded on a Bruker DRX 400 at 278 K at 400 MHz (¹H) and 100 MHz (¹³C) or on a Bruker DRX 500 at 360 K at 500 MHz (¹H). MALDI-TOF MS experiments were carried out on a Bruker Daltonik Reflex III with dithranol (98.5%, Aldrich) as matrix. Elemental analyses were determined with an Elementar Vario *EL*. PXRD-measurements were taken on a PANalytical X'Pert MPD Pro using copper radiation ($K_{\alpha 1} = 1.5405980 \text{ \AA}$). THF was purchased from Prolabo and dried over Na/benzophenone prior to use. Acetonitrile was purchased from Fluka and dried over CaH₂ prior to use. Hexamethylenetetramine (Merck, 99%), 4-*n*-butylphenol (Alfa Aesar, 98%) and trifluoroacetic acid (TFA) (Solvay Fluor GmbH, 99.9%) were used without further purification. Triamine **2**^[S1] was synthesized by a procedure published before.

The surface areas and porosities of cage compounds were characterized by nitrogen adsorption and desorption analysis at 77.35 K with an autosorb computer controlled surface analyzer (AUTOSORB-1 or Quadrasorb from Quantachrome). Each sample was degassed at 200 °C for 23 h before analysed. The Brunauer-Emmett-Teller (BET) surface area was calculated assuming a value of 0.162 nm² for the cross-sectional area of the nitrogen molecules in the pressure range $P/P_0 = 0.01\text{-}0.1$. The nonlinear-differential function theory (NL-DFT model) and isotherm data were used to calculate the pore size distribution. Scanning electron microscopy (SEM) images were obtained on a Zeiss NVision 40 Argon Crossbeam microscope for the observation of morphology of the cage compounds. Thermal gravimetric analyses were measured on a Mettler Toledo TGA/SDTA 851 with a heating rate of 10 °C/min and a nitrogen flow of 50 mL/min.

2,6-diformyl-4-*n*-butylphenol (2c) and 2-formyl-4-*n*-butylphenol: 4-*n*-Butylphenol (3.67 g, 24.4 mmol) and hexamethylenetetramine (HMTA) (7.21 g, 51.4 mmol) were dissolved in

anhydrous trifluoroacetic acid (TFA) (45 mL) under argon and heated under reflux for 24 h. The red solution was cooled to room temperature, poured in 400 mL of a 1:1 mixture of 4 M HCl and dichloromethane (DCM) and was stirred overnight at room temperature. The layers were separated and the aqueous layer extracted twice with dichloromethane (200 mL). The combined organic layer was washed twice with 4 M HCl (200 mL), water (200 mL), brine (200 mL) and dried over sodium sulphate. The solvent was removed by rotary evaporation to give 4.48 g of a yellow liquid. Purification by column chromatography (SiO₂, dichloromethane/light petrol ether = 1:1) gave after drying in vacuum: 1st fraction ($R_f = 0.37$): 1.05 g (24%) of monoaldehyde as a yellow liquid. Refraction index: $n_D^{20} = 1.538$. ¹H NMR (CDCl₃, 400 MHz) δ 10.85 ppm (s, 1H, -OH), 9.87 (s, 1H, -CHO), 7.35 (“dd”, 1H, ⁴ $J = 2.1$ Hz, ³ $J = 8.1$ Hz, Ar-H), 7.34 (s, 1H, Ar-H), 6.91 (d, 1H, ³ $J = 8.1$ Hz, Ar-H), 2.60 (t, 2H, ³ $J = 7.6$ Hz, -CCH₂CH₂CH₂CH₃), 1.62-1.55 (m, 2H, -CCH₂CH₂CH₂CH₃), 1.40-1.31 (m, 2H, -CCH₂CH₂CH₂CH₃), 0.93 (t, 3H, ³ $J = 7.3$ Hz, -CCH₂CH₂CH₂CH₃). The analytical data are in accordance to those previously described.^[S2] 2nd fraction ($R_f = 0.13$): 2.58 g (51%) of dialdehyde **2c** as a pale yellow solid: mp 58 °C. ¹H NMR (400 MHz, CDCl₃) δ 11.46 (s, 1H, -OH), 10.22 (s, 2H, -CHO), 7.77 (s, 2H, -ArH), 2.64 (t, 2H, ³ $J = 7.7$ Hz, Ar-CH₂), 1.65 - 1.57 (m, 2H, Ar-CH₂CH₂), 1.40 - 1.31 (m, 2H, Ar-CH₂CH₂CH₂), 0.94 (t, ³ $J = 7.3$ Hz, 3H, -CH₃). ¹³C NMR (CDCl₃, 100 MHz) δ 192.3 ppm (d, -CHO), 162.1 (s, Ar-COH), 137.5 (s, Ar-C-CH₂), 134.8 (d, Ar-C-H), 123.1 (s, Ar-C-CHO), 34.3 (t, Ar-CH₂), 33.4 (t, Ar-CH₂-CH₂), 22.3 (t, -CH₂CH₃), 14.0 (q, -CH₃). IR (KBr): 3435 (m), 3027 (m), 2956 (s), 2937 (s), 2874 (s), 2857 (s), 2783 (w), 1685 (s), 1651 (s), 1600 (s), 1533 (w), 1455 (s), 1406 (m), 1384 (m), 1339 (m), 1331 (m), 1309 (s), 1264 (s), 1217 (s), 1155 (w), 1103 (w), 1007 (w), 980 (s), 971 (s), 915 (m), 887 (w), 812 (m), 768 (s), 749 (s), 648 (s), 608 (s), 556 (w), 510 (m), 442 (w) cm⁻¹. MS (CI-MS) m/z (%) 235 (15) [M+C₂H₆]⁺, 208 (13), 207 (100) [M+H]⁺. Analysis calcd. for C₁₂H₁₄O₃: C 69.88, H 6.84; found: C 69.64, H 6.71.

Cage compound 3c^B: Triamine **1** (122 mg, 0.408 mmol) and salicyldialdehyde **2e** (127 mg, 0.616 mmol) were dissolved under argon in dry THF (43 mL), dry acetonitrile (26 mL) and TFA (28.2 μ L, 2 mol%) were added and the reaction mixture was refluxed in an apparatus connected with a dropping funnel with molecular sieves 4 Å. After two days the mixture was cooled to room temperature and the precipitate was collected on a Büchner-funnel, washed with a NEt₃/THF-solution (50 μ L of NEt₃ in 5 mL THF), dry THF (2 x 5 mL), and *n*-pentane (2 x 5 mL) and dried in vacuum. 128 mg (56%) of **3c^B** was obtained as an orange solid. Mp. > 410 °C. ¹H NMR (DMSO-d₆, 400 MHz, 360 K) δ 13.70 ppm (s, 6H, -OH), 9.11 (s, 12H, -

NCH), 7.81 (s, 12H, Ar-*H*), 7.69 (d, 12H, $^4J = 1.7$ Hz, Ar-*H*), 7.58 (d, 12H, $^3J = 7.9$ Hz, Ar-*H*), 7.25 (dd, 12H, $^4J = 1.9$ Hz, $^3J = 7.8$ Hz, Ar-*H*), 5.99 (s, 4H, bridgehead-*H*), 5.77 (s, 4H, bridgehead-*H*), 2.54 (m, 12H, -CCH₂CH₂CH₂CH₃), 1.62-1.58 (m, 12H, -CCH₂CH₂CH₂CH₃), 1.46-1.32 (m, 12H, -CCH₂CH₂CH₂CH₃), 0.91 (t, 18H, $^3J = 7.8$ Hz, -CCH₂CH₂CH₂CH₃). ¹³C NMR (125 MHz, THF-*d*₈) δ 160.5 ppm, 148.1, 147.7, 145.3, 134.2, 125.1, 55.3, 54.2, 35.6, 34.9, 23.3, 14.4. IR (KBr): 3435 (m), 2955 (m), 2927 (m), 2857 (w), 1683 (w), 1624 (s), 1581 (s), 1467 (s), 1379 (w), 1312 (w), 1261 (w), 1223 (w), 1158 (m), 1022 (m), 952 (w), 857 (m), 782 (w), 761 (w), 653 (w), 594 (w), 477 (w) cm⁻¹. MS (MALDI-TOF, dithranol) *m/z* 2218.3. Analysis calcd. for C₁₅₂H₁₂₈N₁₂O₆·3CH₃CN: C 81.03, H 5.90; N 8.97; found: C 81.15, H 5.72, N 8.91.

Cage compound 3c^{cr}: Crystalline material was obtained by dissolving cage compound **3c** in dry THF, followed by filtering the suspension through a 25 mm syringe filter (0.45 μ m PTFE) and vapour diffusion of acetonitrile in the THF-solution. The crystalline material was separated via pipette technique. Analytical data are in accordance to those above.

Cage compound 3a^B was synthesized as described above for **3c^B**: Triamine **1** (80.6 mg, 0.27 mmol) and salicyldialdehyde **2a** (102 mg, 0.41 mmol) were dissolved under argon in dry THF (19 mL), dry acetonitrile (26 mL) and TFA (18.3 μ L, 2 mol%) were added. After three days the mixture was cooled to room temperature and the precipitate was collected, washed with a NEt₃/THF-solution (50 μ L of NEt₃ in 5 mL THF), dry THF (2 x 5 mL), pentane (2 x 5 mL) and dried in vacuum. 123 mg (73%) of **3a^B** was obtained as an orange solid. Analytical data are in accordance to those of **3a^A**.^[S3]

Cage compound 3b^B was synthesized as described above for **3c^B**: Triamine **1** (70.5 mg, 0.24 mmol) and salicyldialdehyde **2b** (139 mg, 0.35 mmol) were dissolved under argon in dry THF (22 mL), dry acetonitrile (22 mL) and TFA (16 μ L, 2 mol%) were added. After three days the mixture was cooled to room temperature and the precipitate was collected, washed with a NEt₃/THF-solution (50 μ L of NEt₃ in 5 mL THF), dry THF (2 x 5 mL), pentane (2 x 5 mL) and dried in vacuum. 143 mg (72%) of **3b^B** was obtained as an orange solid. Analytical data are in accordance to **3b^A**.^[S3]

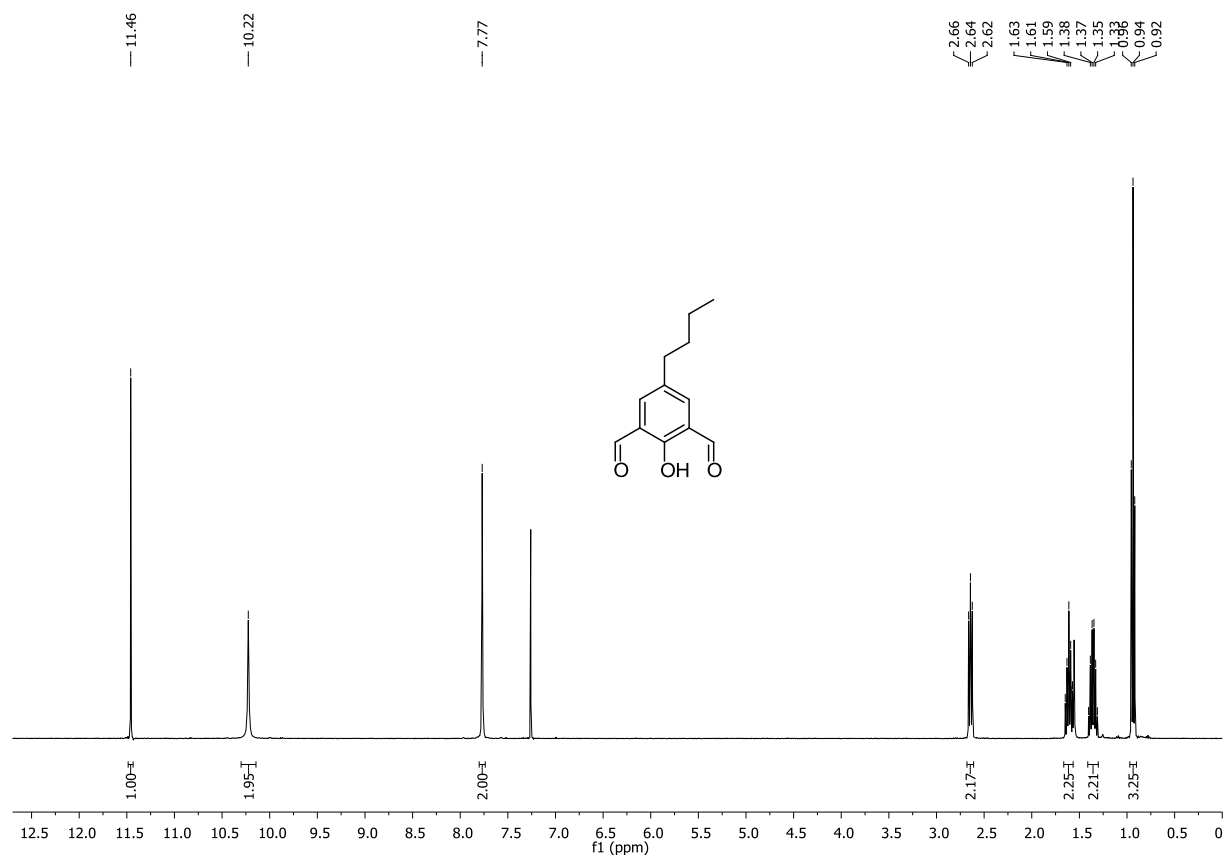


Figure S1: ¹H NMR spectrum (CDCl₃, 400 MHz) of 2,6-Diformyl-4-*n*-butylphenol **2c**.

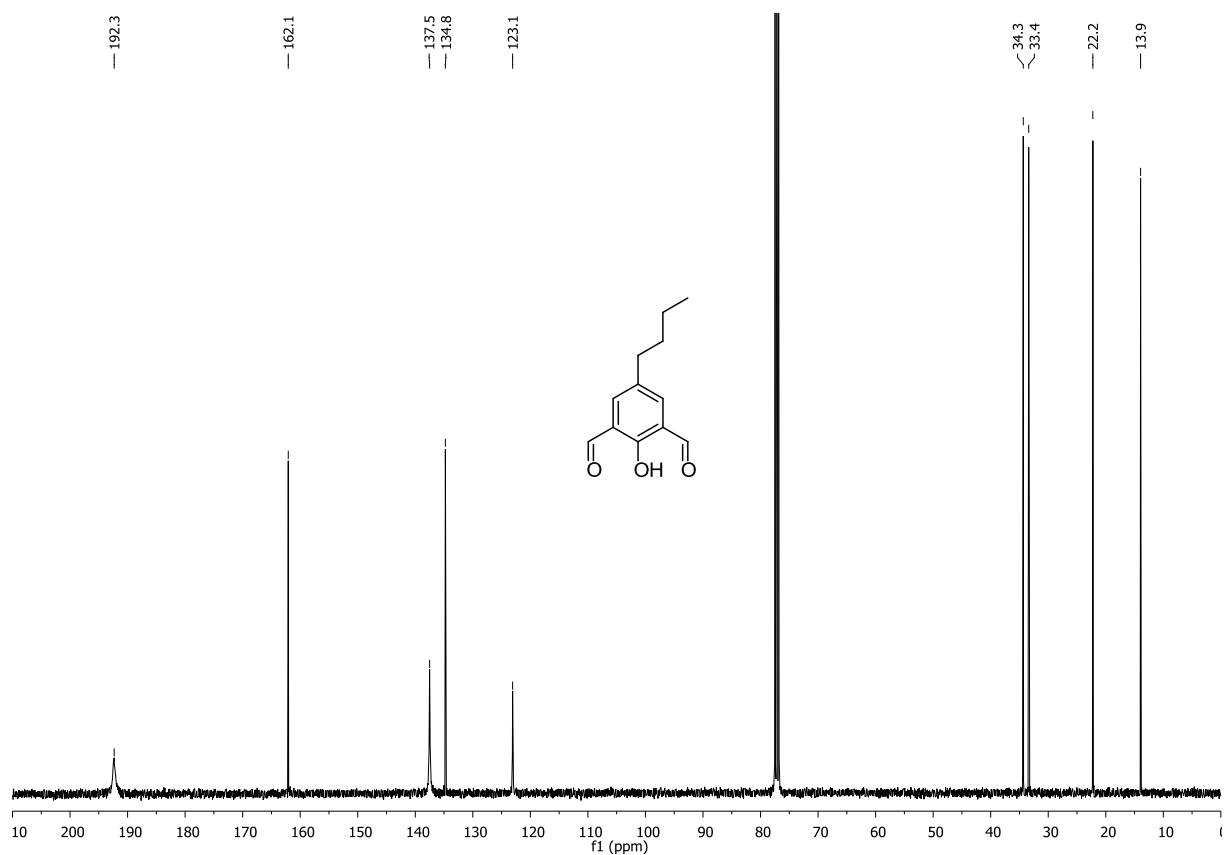


Figure S2: ¹³C NMR spectrum (CDCl₃, 100 MHz) of 2,6-Diformyl-4-*n*-butylphenol **2c**.

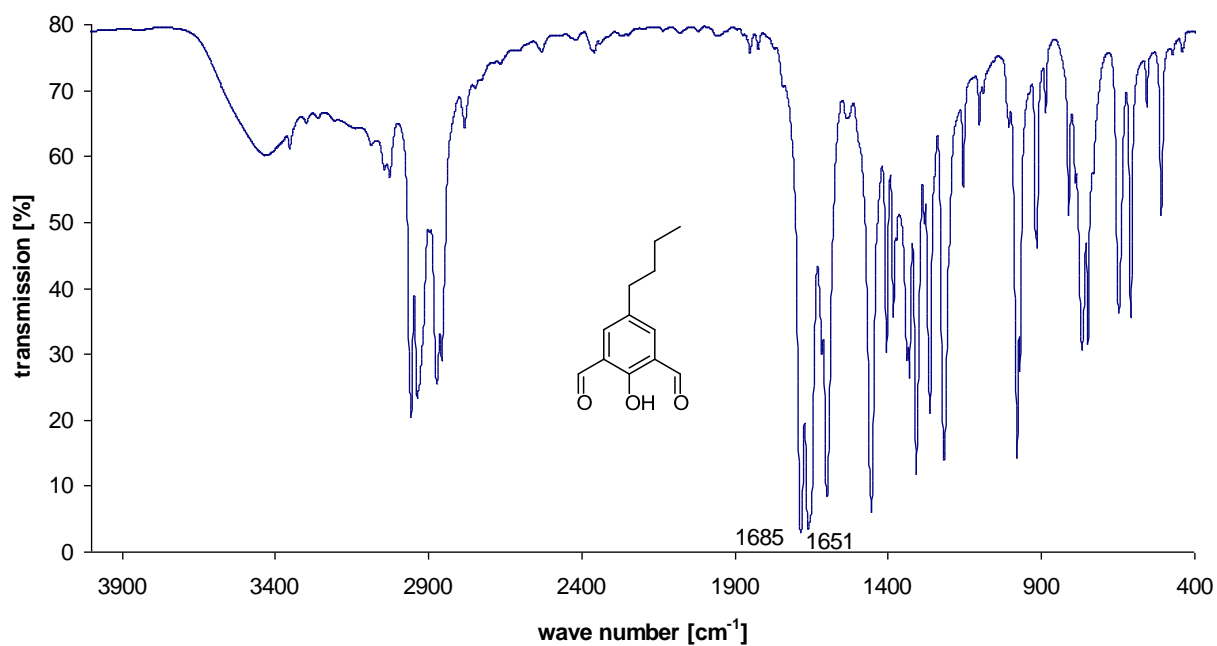


Figure S3: FT-IR spectrum (KBr) of 2,6-Diformyl-4-*n*-butylphenol **2c**.

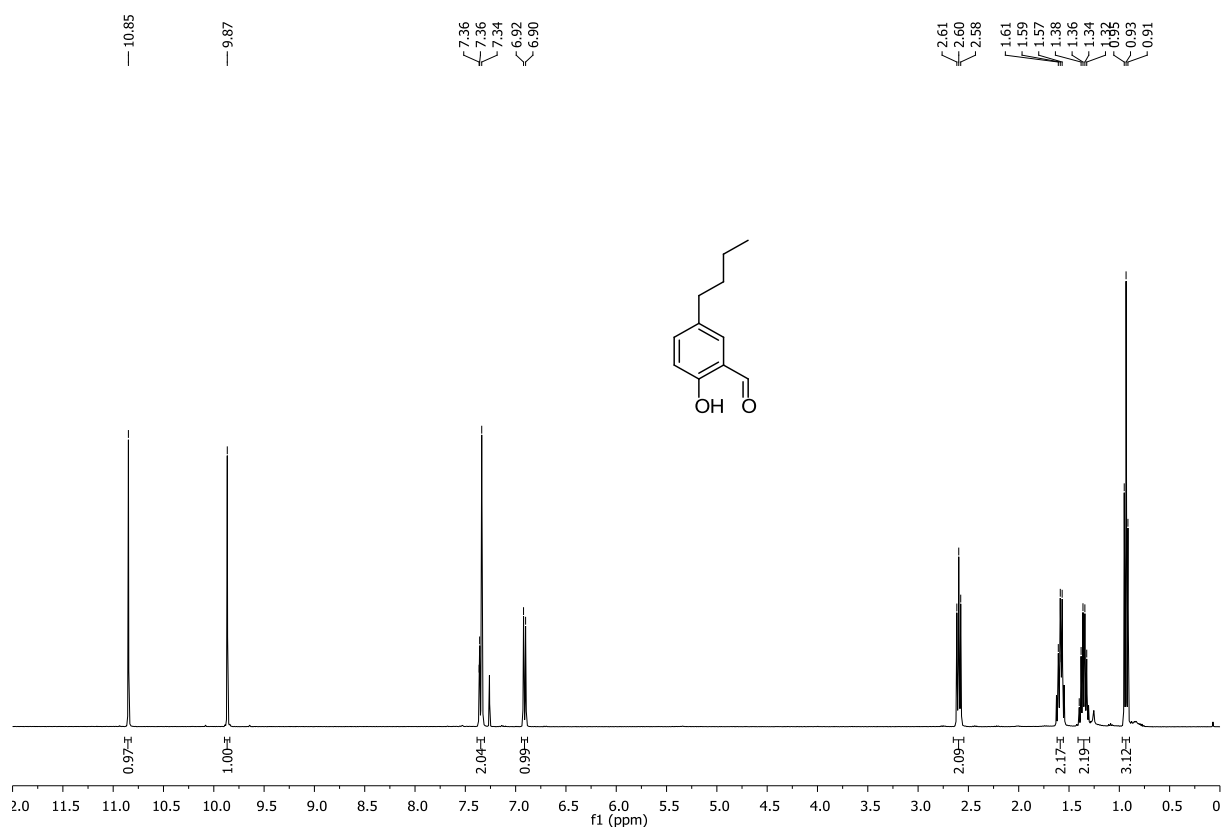


Figure S4: ¹H NMR spectrum (CDCl₃, 400 MHz) of 2-formyl-4-*n*-butylphenol.

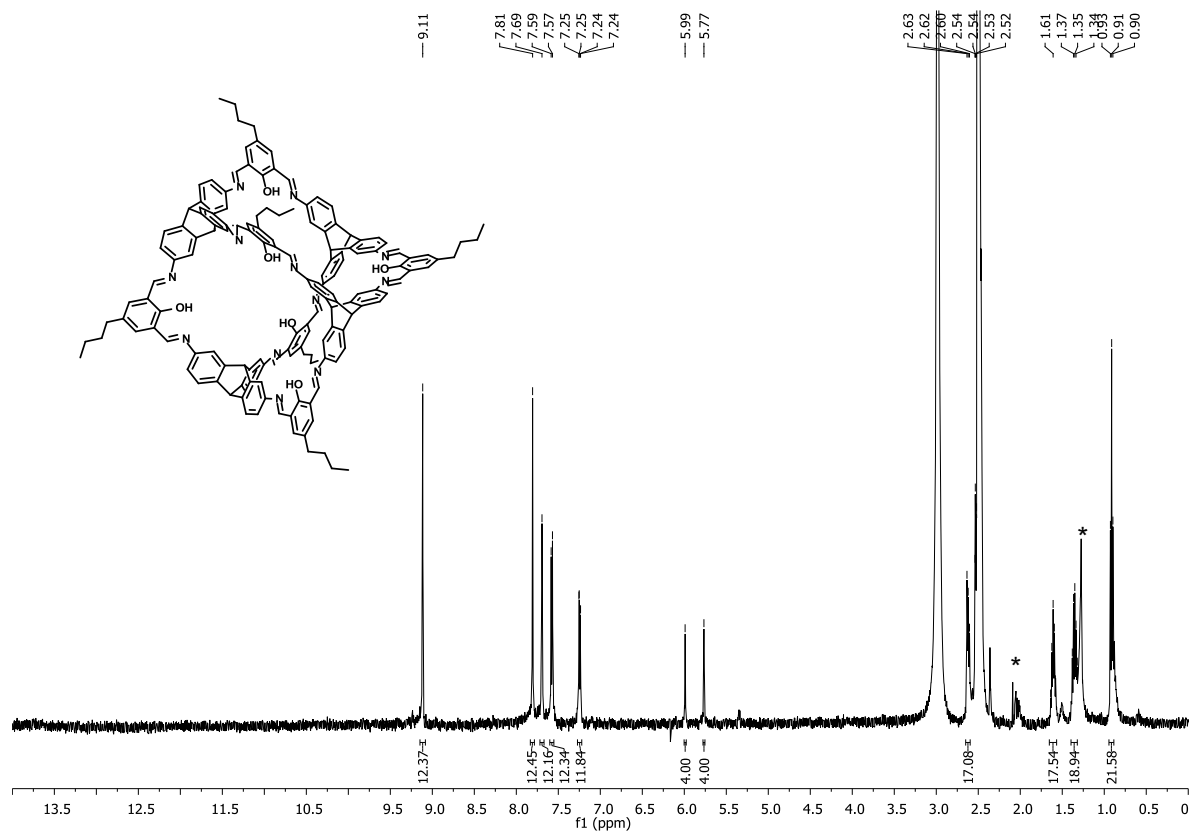


Figure S5: ¹H NMR (DMSO-d₆, 400 MHz, 360 K) of cage compound **3c^B**. The asterisks mark residual solvent peaks (n-pentane, acetonitrile).

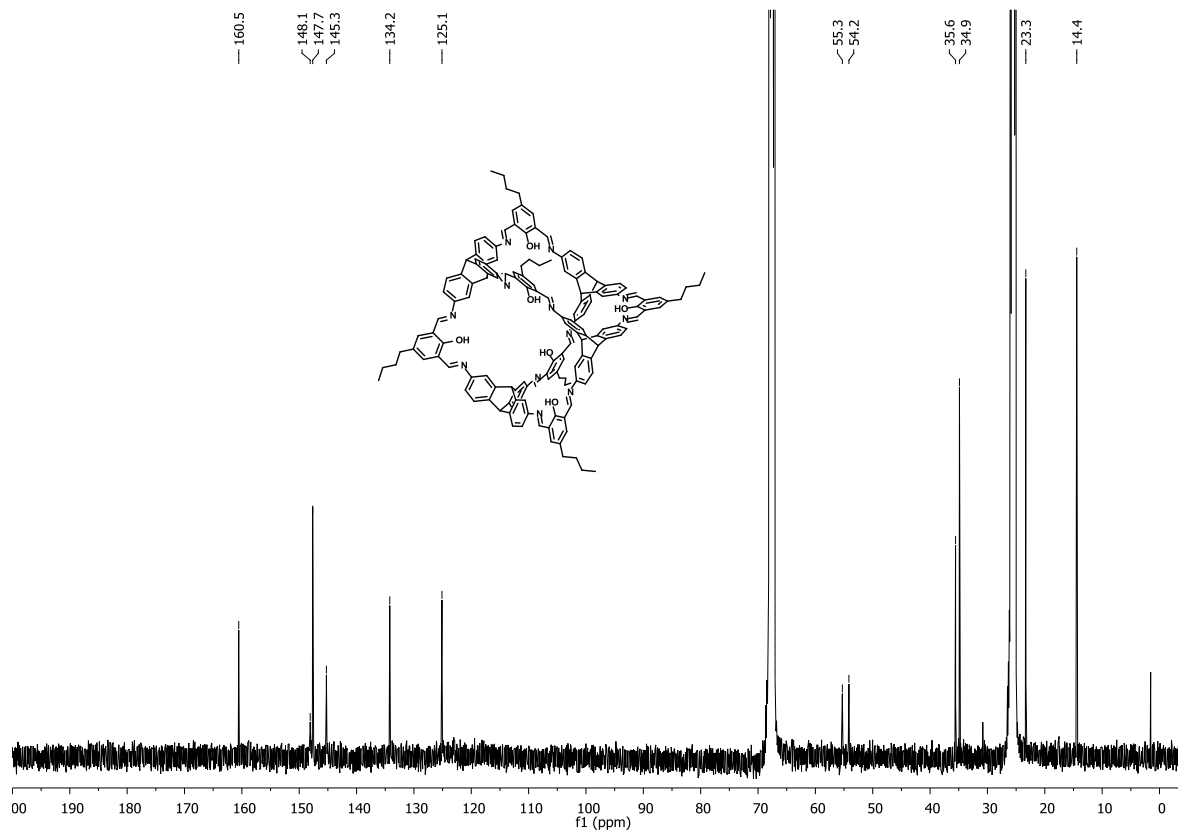


Figure S6: ¹³C NMR (THF-d₈, 125 MHz, 301 K) of cage compound **3c^B**.

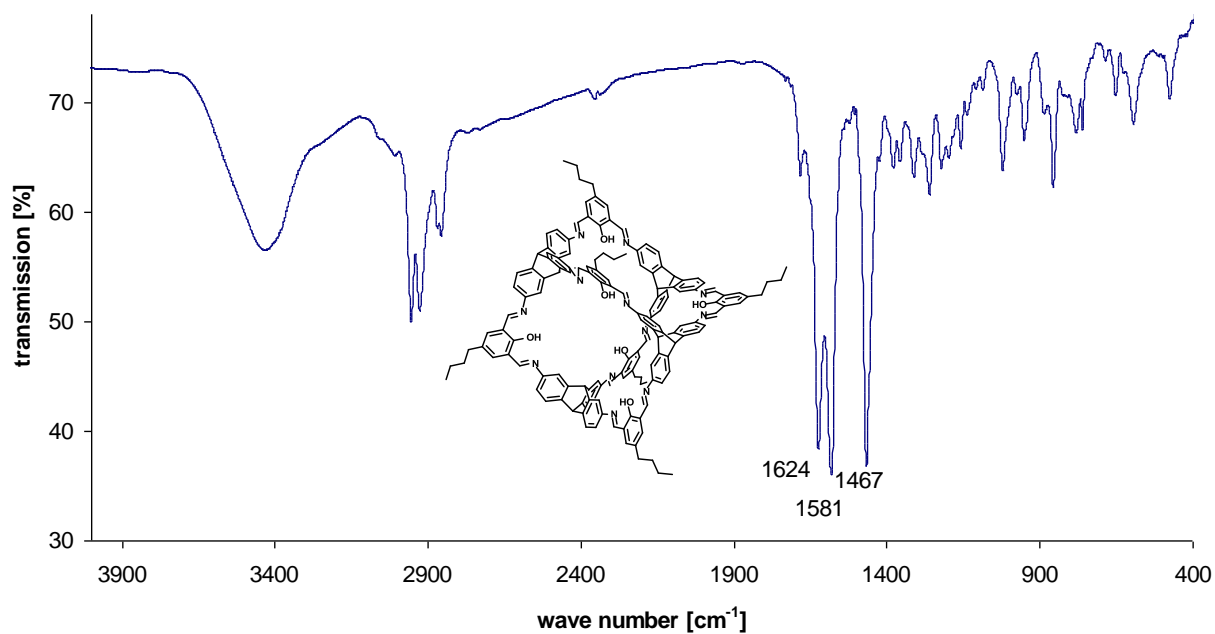


Figure S7: FT-IR spectrum (KBr) of cage compound **3c^B**.

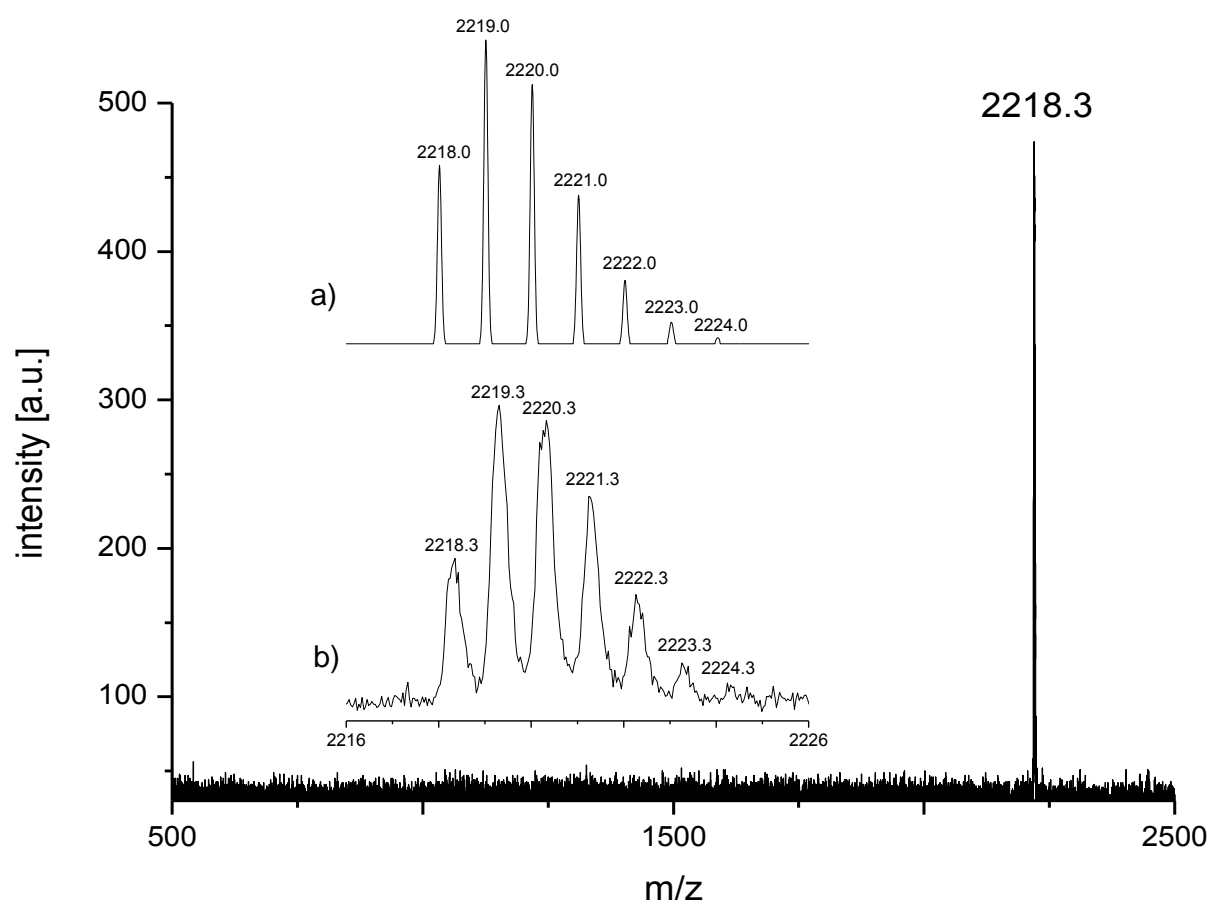


Figure S8: MALDI-TOF MS (dithranol) of cage compound **3c^B**. a) Calculated isotopic pattern for **3c+H⁺** and b) zoomed in section of the mass peak.

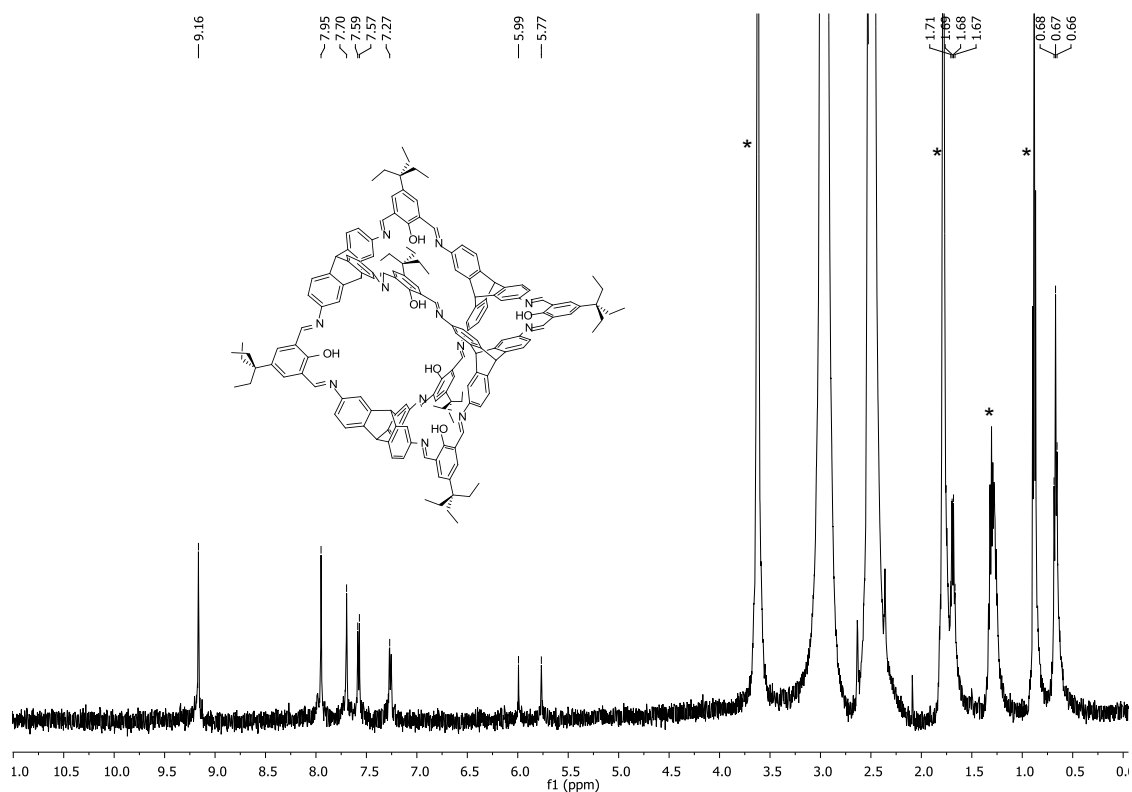


Figure S9: ¹H NMR (DMSO-d₆, 400 MHz, 360 K) of cage compound **3a^B**. The asterisks mark residual solvent peaks (n-pentane, acetonitrile and THF). Data are in accordance to those published before.^[S3]

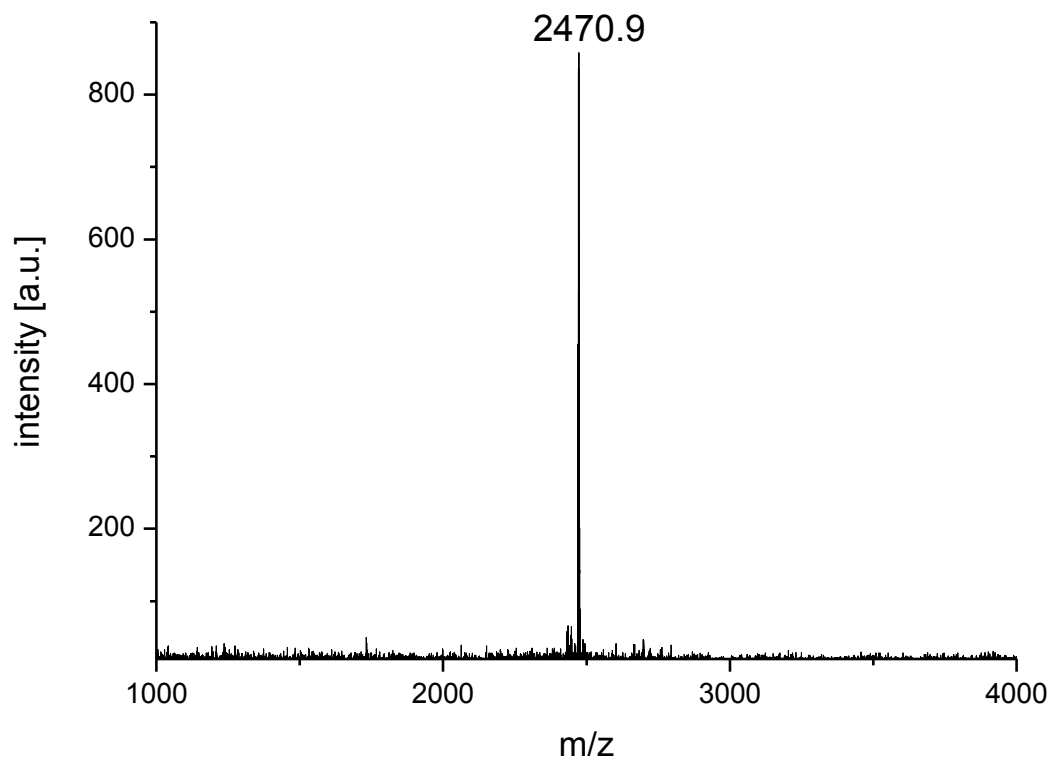


Figure S10: MALDI-TOF MS (dithranol) of cage compound **3a^B**. Data are in accordance to those published before.^[S3]

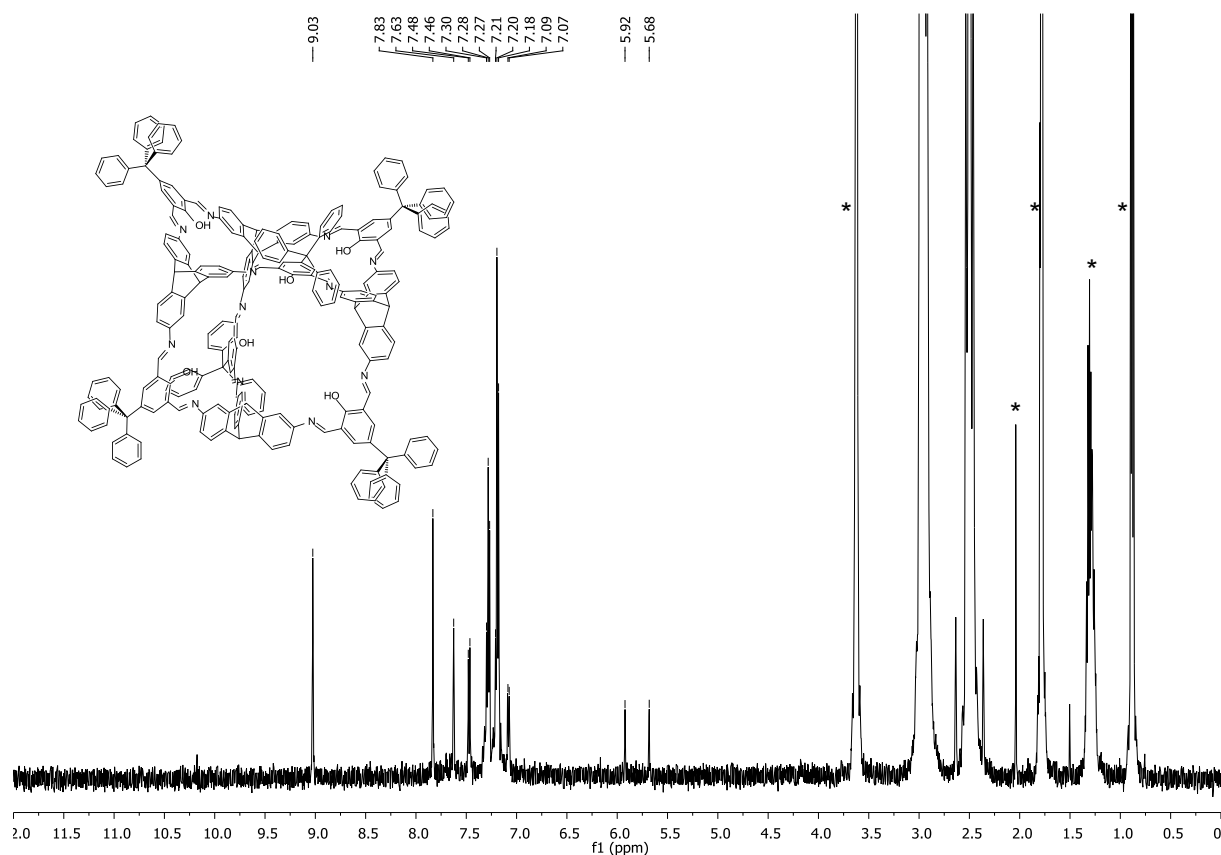


Figure S11: ^1H NMR (DMSO- d_6 , 400 MHz, 360 K) of cage compound **3b^B**. The asterisks mark residual solvent peaks (n-pentane, acetonitrile, THF). Data are in accordance to those published before.^[S3]

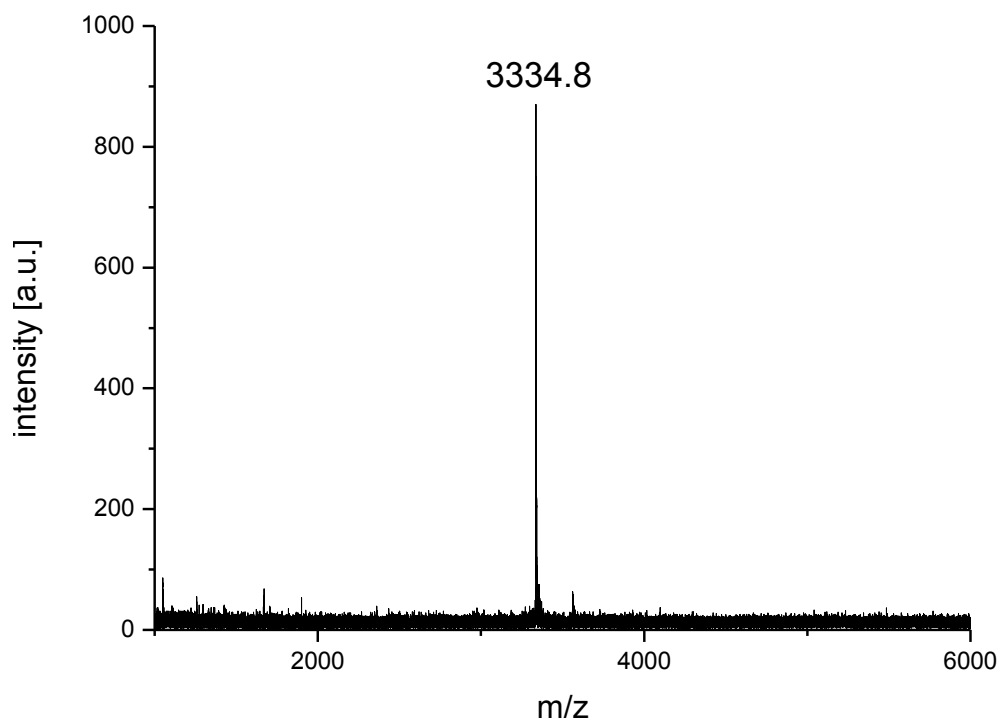


Figure S12: MALDI-TOF MS (dithranol) of cage compound **3b^B**. Data are in accordance to those published before.^[S3]

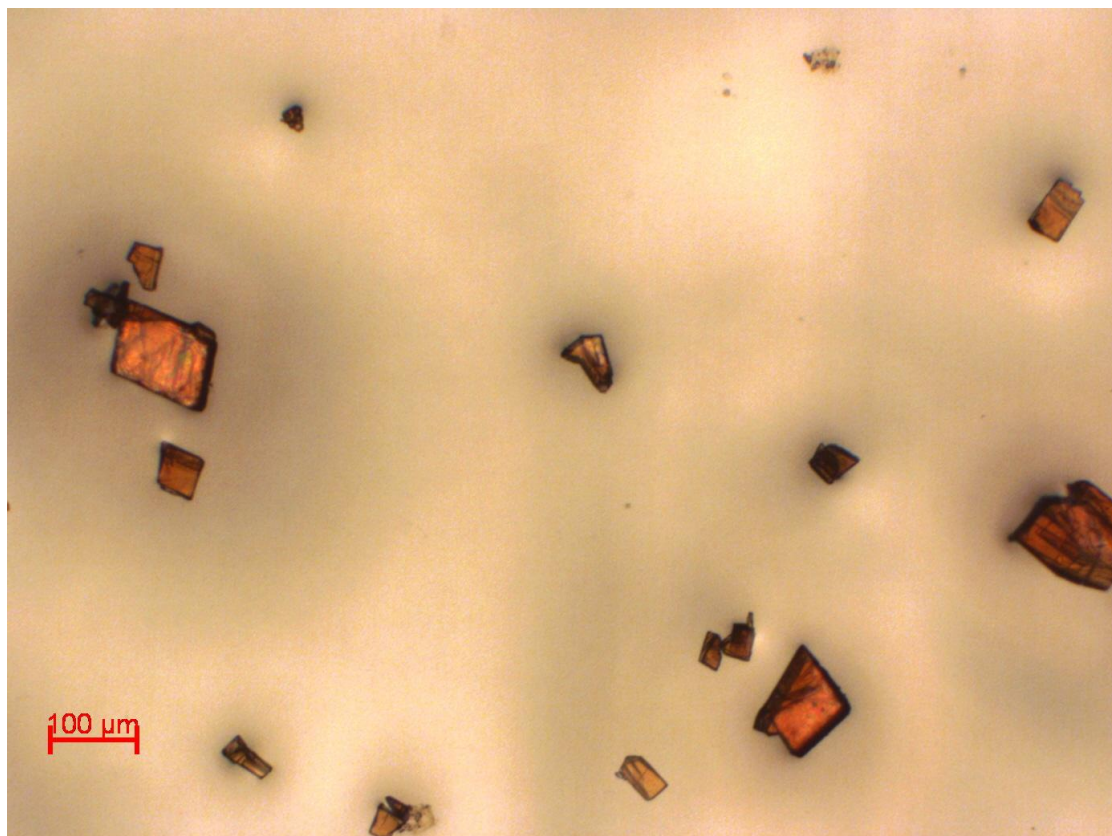


Figure S13: Light microscope image of crystalline material of cage compound $3c^{cr}$.

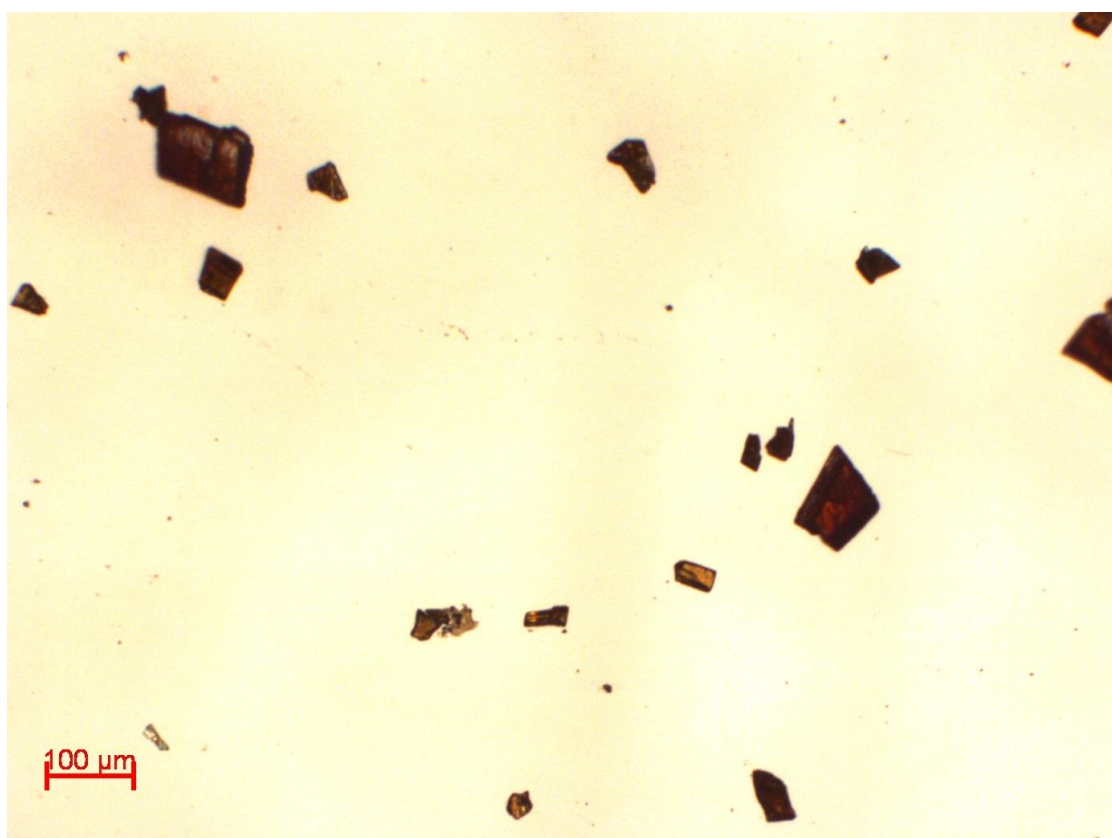


Figure S14: Light microscope image of crystalline material of cage compound $3c^{cr}$ after 20 seconds.

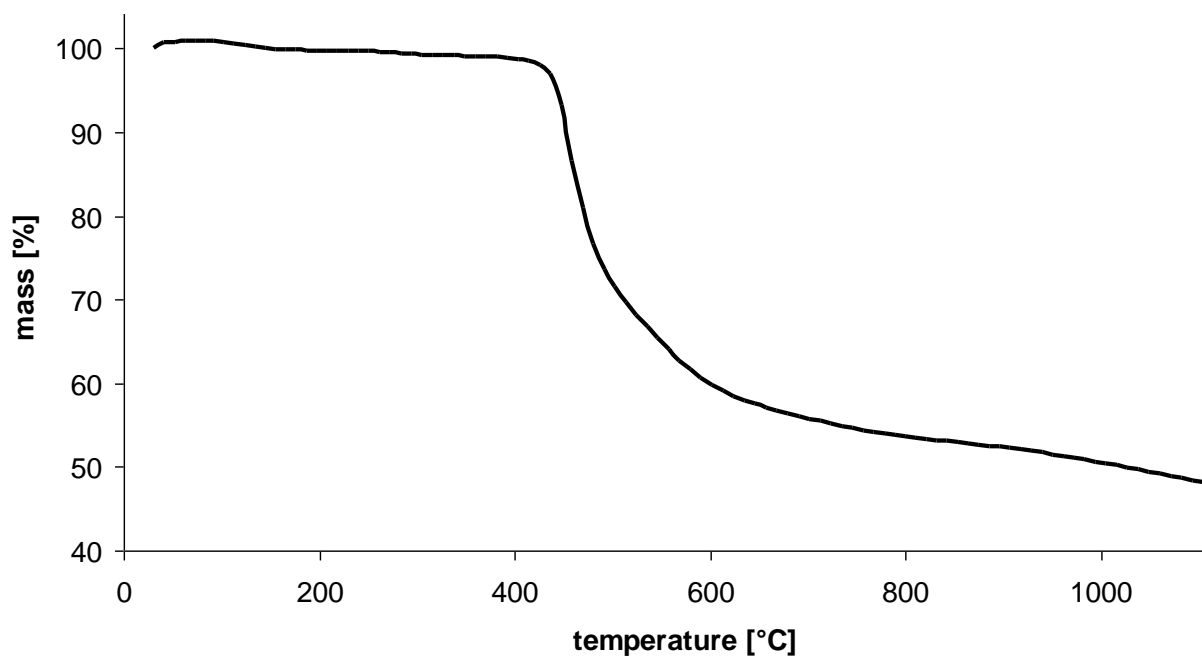


Figure S15: TGA measurement of as-synthesized material of cage compound **3c^B**.

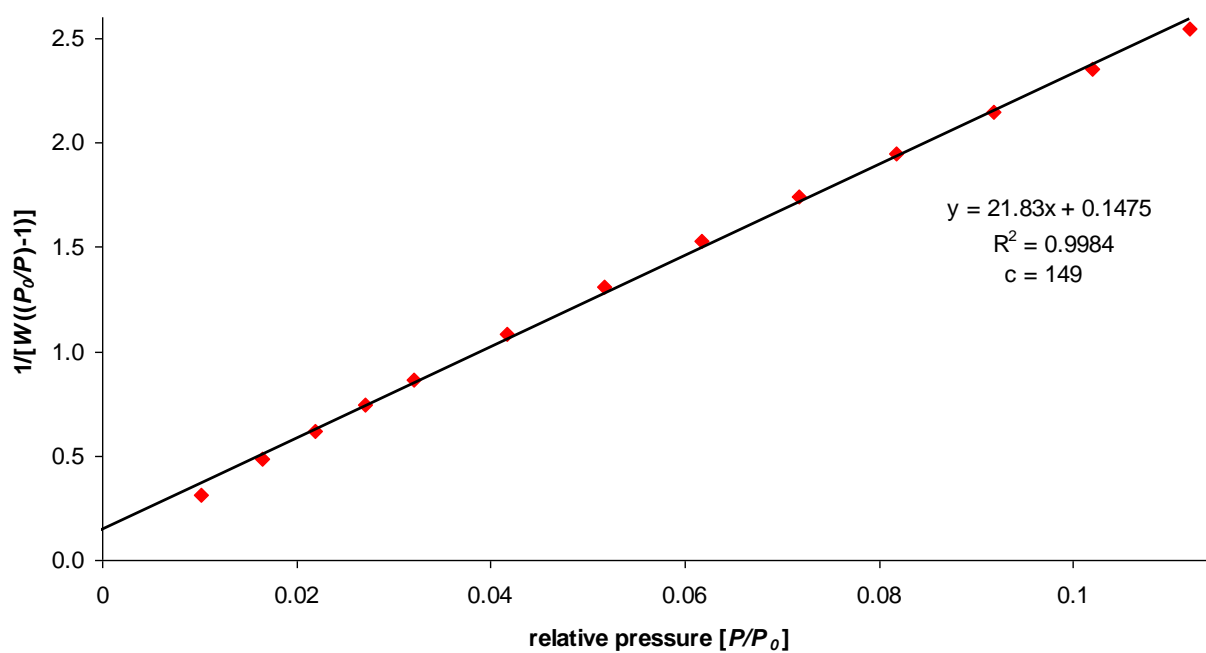


Figure S16: BET plot of as-synthesized material of cage compound **3c^B**.

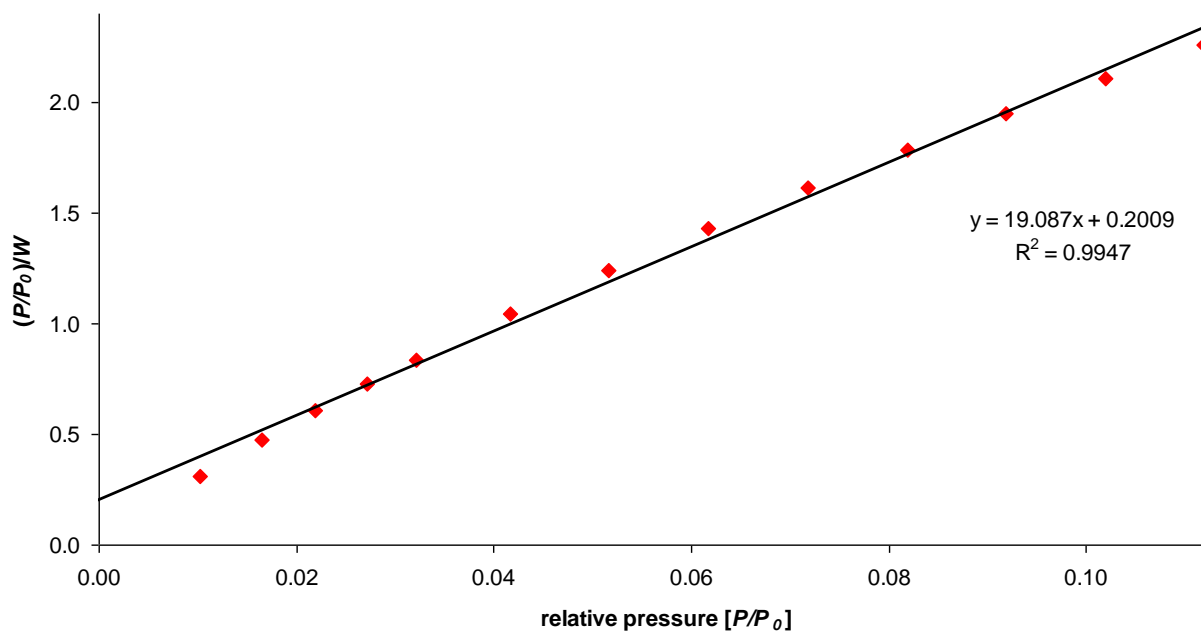


Figure S17: Langmuir plot of as-synthesized material of cage compound **3c^B**.

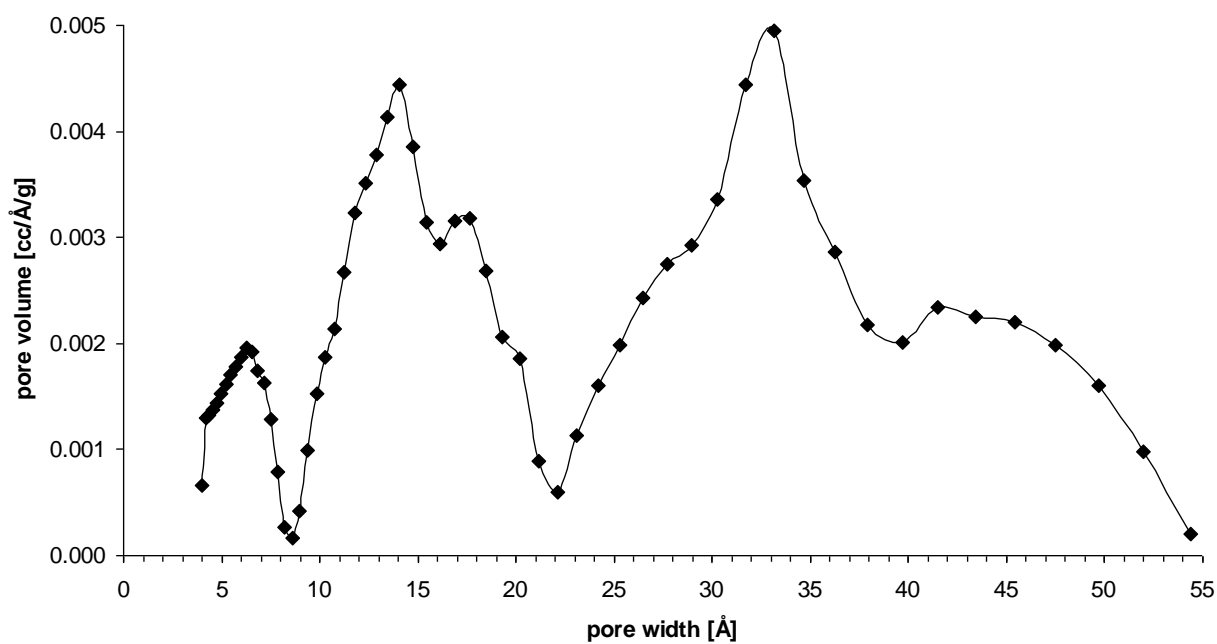


Figure S18: NL-DFT pore size distribution of as-synthesized material of cage compound **3c^B**.

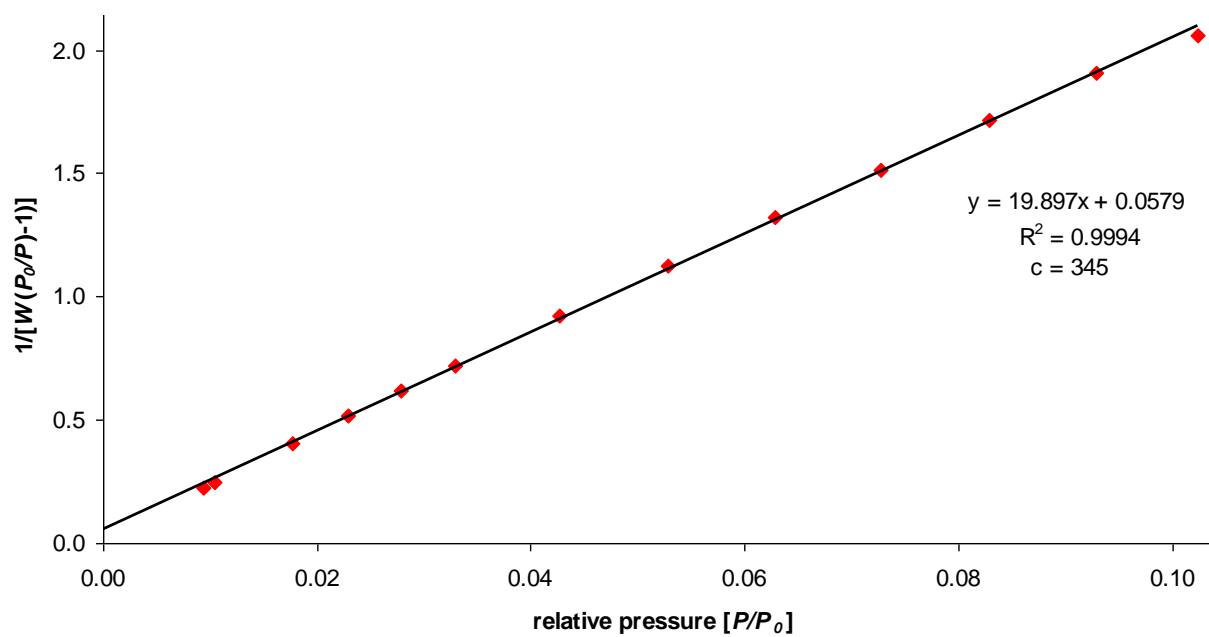


Figure S19: BET plot of crystalline material of cage compound $3c^{cr}$.

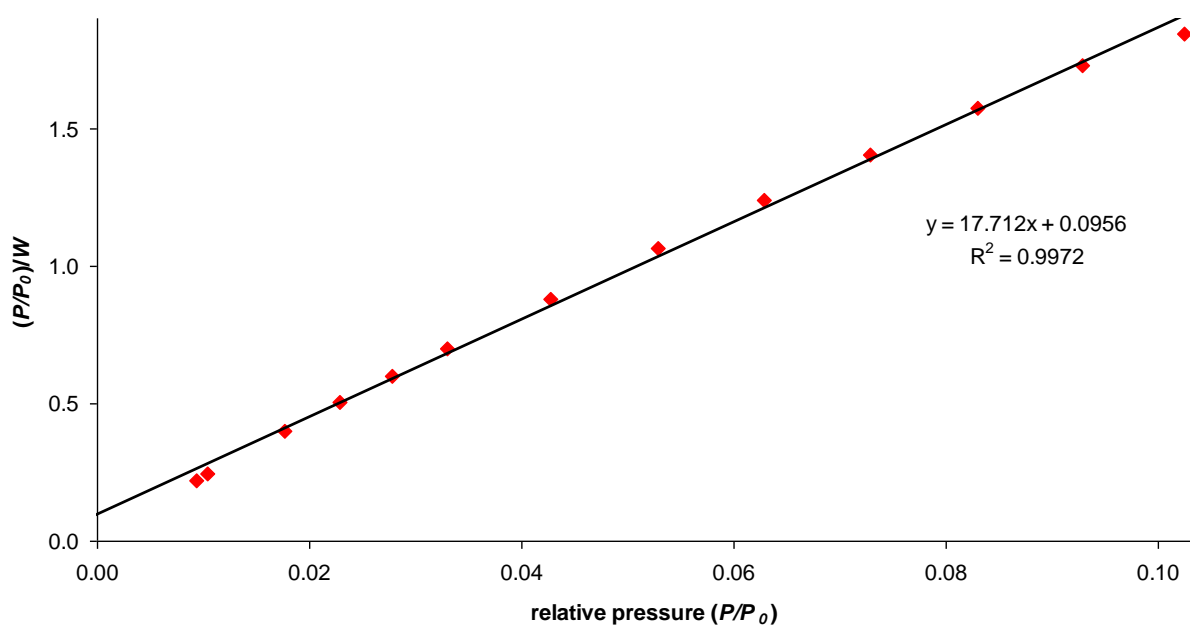


Figure S20: Langmuir plot of crystalline material of cage compound $3c^{cr}$.

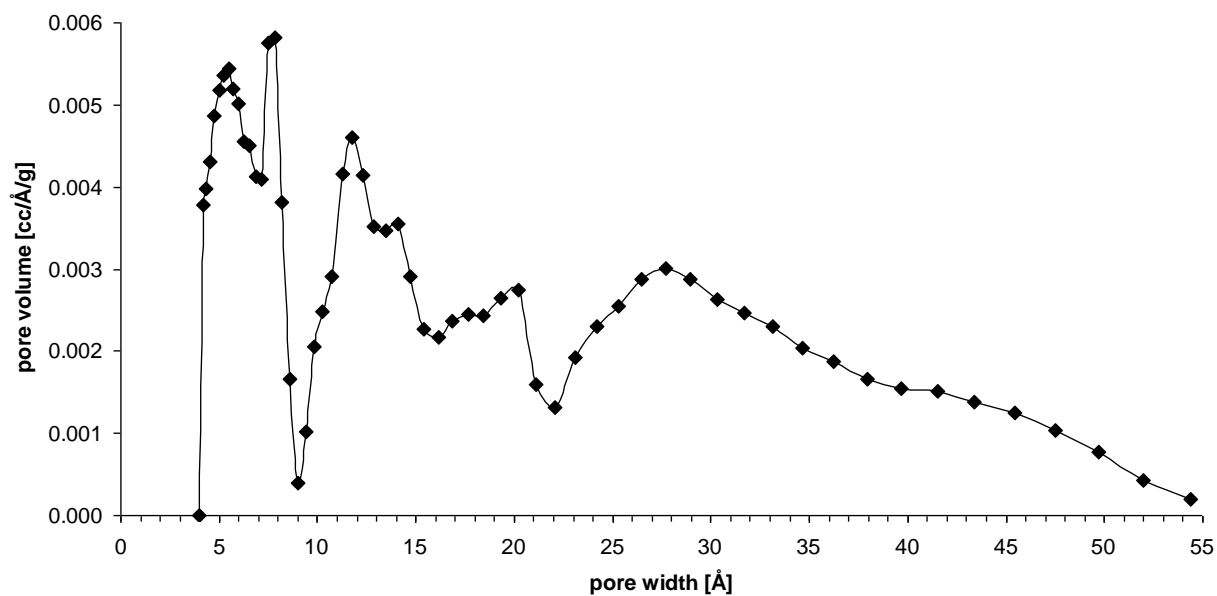


Figure S21: NL-DFT pore size distribution of crystalline material of cage compound $3c^{cr}$.

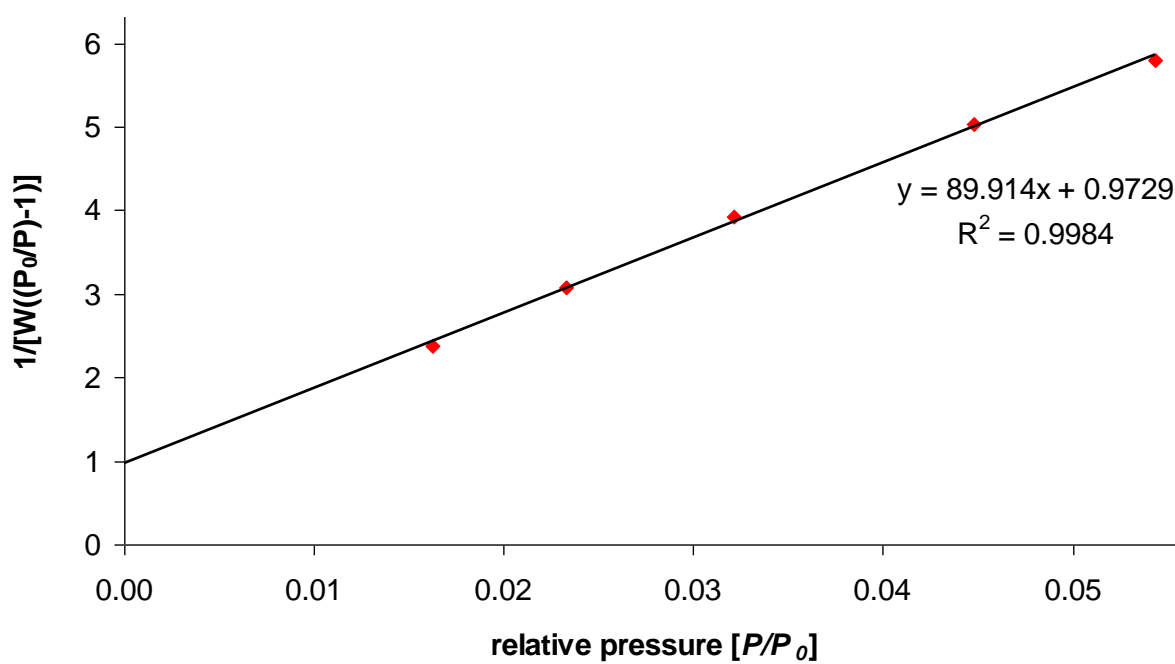


Figure S22: BET plot of cage compound $3a^B$.

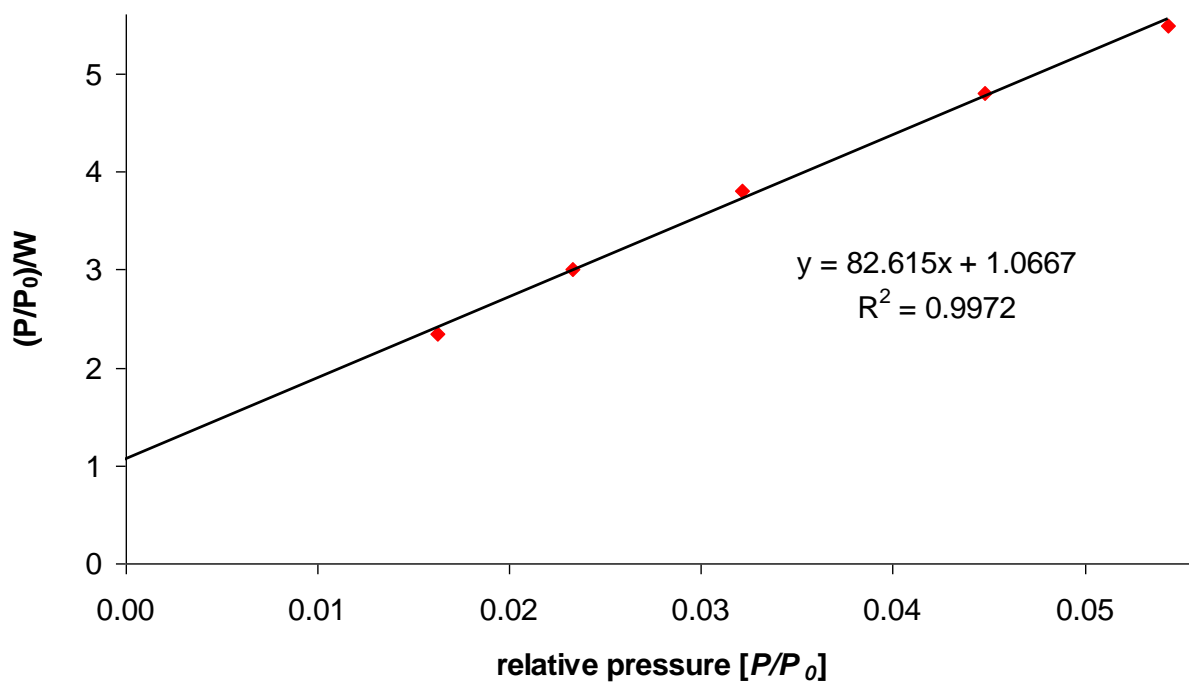


Figure S23: Langmuir plot of cage compound **3a^B**.

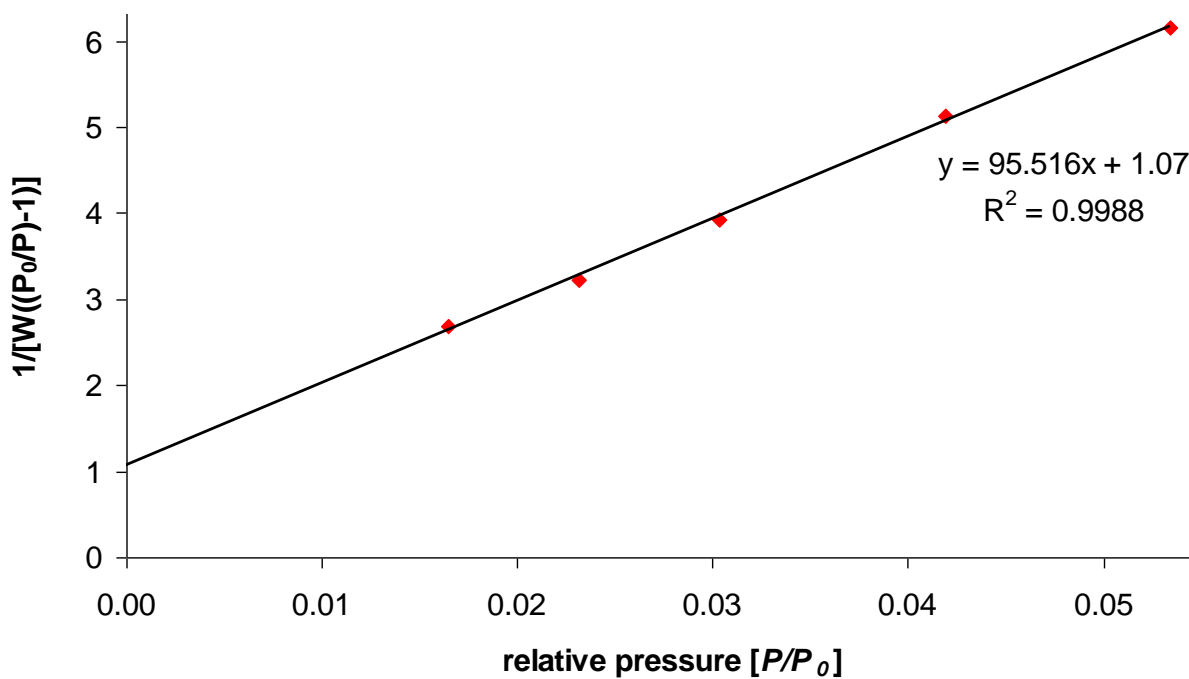


Figure S24: BET plot of cage compound **3b^B**.

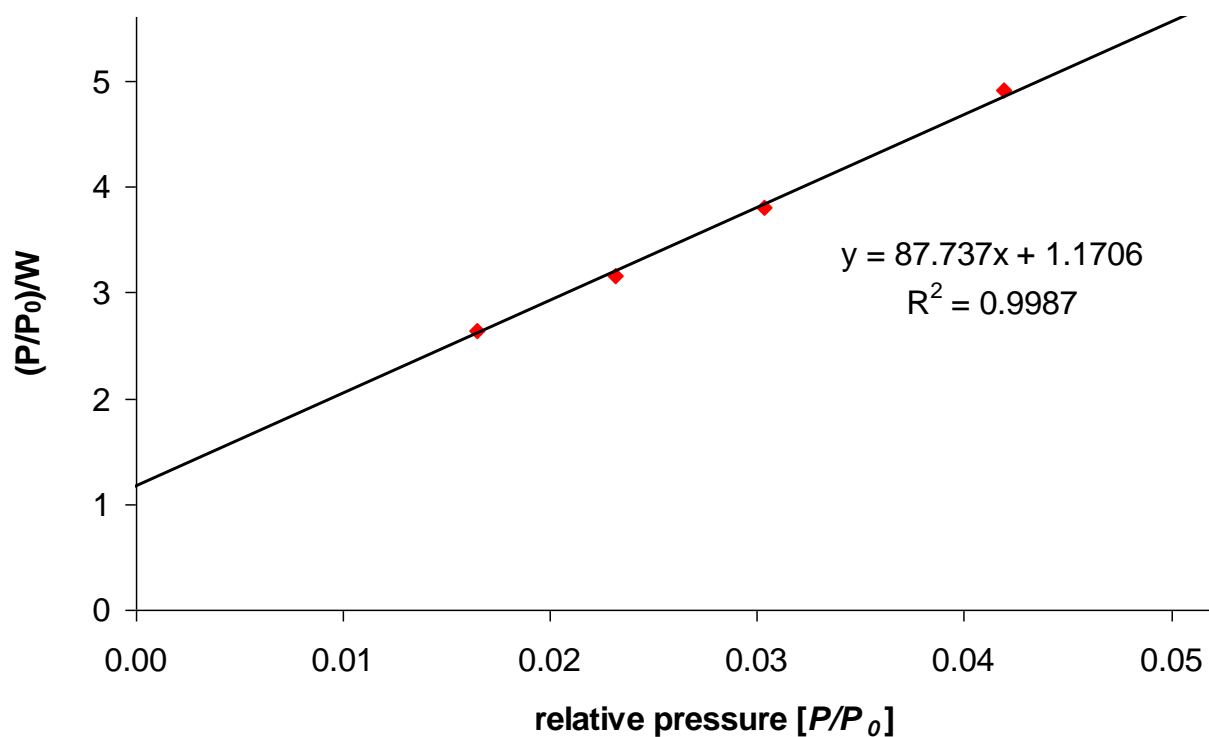


Figure S25: Langmuir plot of cage compound $3b^B$.

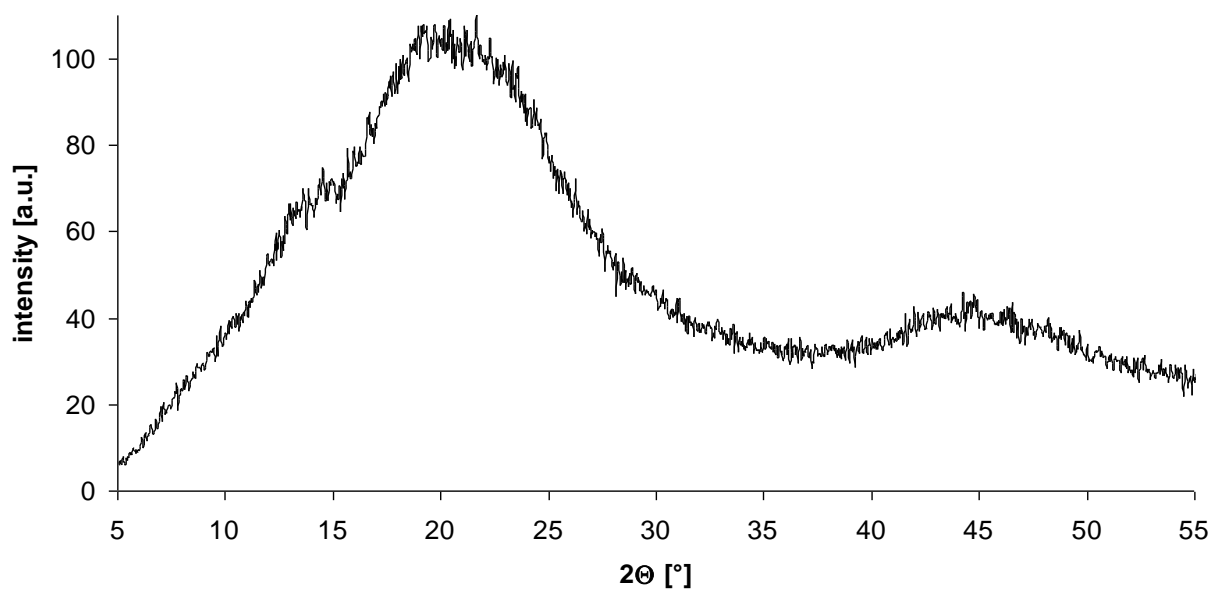


Figure S26: PXRD measurement of as-synthesized material of cage compound $3c^B$ after BET measurement.

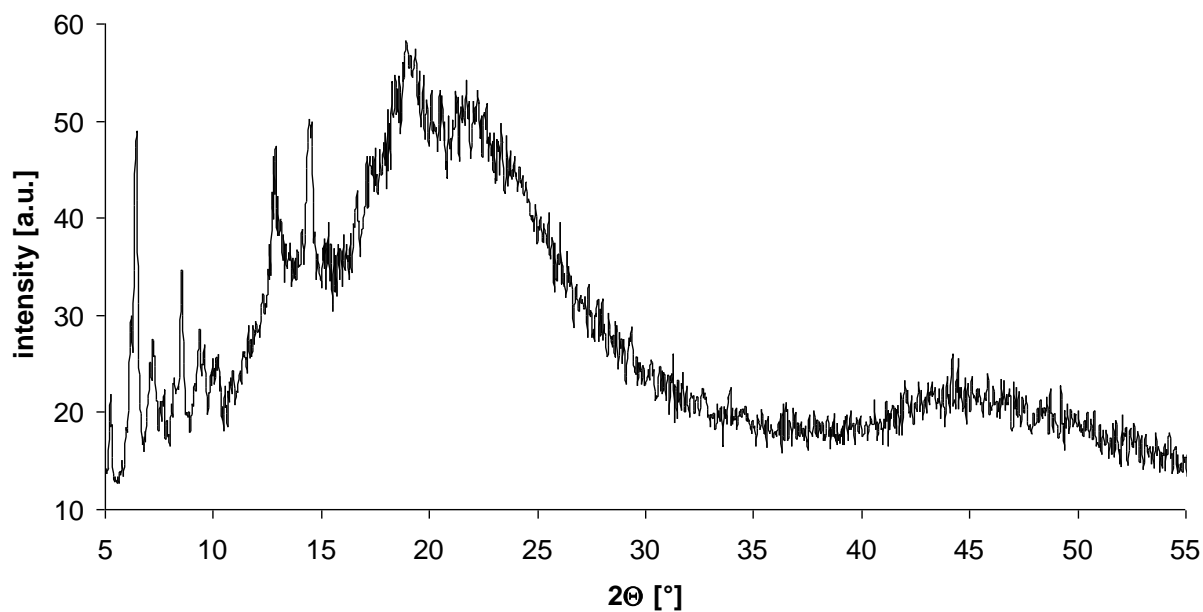


Figure S27: PXRD measurement of crystalline material of cage compound $3c^{cr}$ after BET measurement.

References:

- [S1] C. Zhang, C.-F. Chen, *J. Org. Chem.* **2006**, *71*, 6626-6629.
- [S2] H.-X. Sun, Z.-H. Sun, B. Wang, *Tetrahedron* **2009**, *50*, 1596-1599.
- [S3] M. W. Schneider, I. M. Oppel, H. Ott, L. G. Lechner, H.-J. S. Hauswald, R. Stoll, M. Mastalerz, *Chem. Eur. J.* **2012**, , DOI: 10.1002/chem.201102857.